

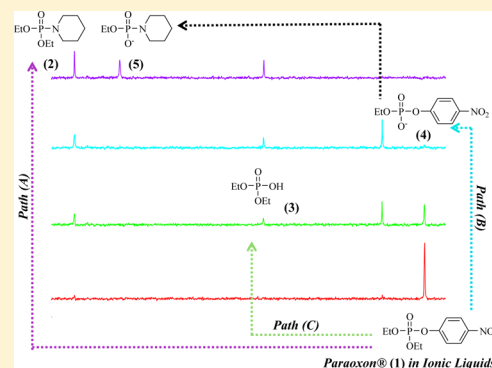
# Mechanisms of Degradation of Paraoxon in Different Ionic Liquids

Paulina Pavez,\* Daniela Millán, Javiera I. Morales, Enrique A. Castro, Claudio López A., and José G. Santos

Facultad de Química, Pontificia Universidad Católica de Chile, Casilla 306, Santiago 6094411, Chile

## Supporting Information

**ABSTRACT:** Herein, the reactivity and selectivity of the reaction of *O,O*-diethyl 4-nitrophenyl phosphate triester (Paraoxon, **1**) with piperidine in ionic liquids (ILs), three conventional organic solvents (COS), and water is studied by <sup>31</sup>P NMR, UV–vis, and GC/MS. Three phosphorylated products are identified as follows: *O,O*-diethyl piperidinophosphate diester (**2**), *O,O*-diethyl phosphate (**3**), and *O*-ethyl 4-nitrophenyl phosphate diester (**4**). Compound **4** also reacts with piperidine to yield *O*-ethyl piperidinophosphate monoester (**5**). The results show that both the rate and products distribution of this reaction depend on peculiar features of ILs as reaction media and the polarity of COS.



## INTRODUCTION

Organophosphorus pesticides (OPs) are widely used worldwide due to their high insecticidal activity and other biological activities.<sup>1</sup> Overall, OPs compounds represent 38% of total pesticides used globally. The higher toxicity of OPs insecticide is attributed to irreversible inhibition of the acetylcholinesterase enzyme, which is essential for central nervous system function in vertebrates and invertebrates; thus they often lack selectivity between nontarget organisms and insect pest.<sup>2</sup> On the other hand, the growing use of these insecticides has increased the risks of environmental contamination of soils and groundwater. Therefore, due to the high toxicity and bioaccumulation shown by these organophosphate compounds, many methods have been developed for their degradation.<sup>1,3</sup> Currently, the available approaches for OPs degradation are homogeneous and heterogeneous hydrolysis,<sup>4</sup> photolysis,<sup>5</sup> photochemical degradation,<sup>6</sup> and biodegradation,<sup>7</sup> as well as chemical treatments based on the use of strong oxidants or nucleophiles.<sup>1,3,8</sup> Nevertheless, some of these treatments may not be very efficient or are unfriendly to the environment due to the formation of products that have mild or acute toxicity.<sup>6,9</sup>

However, it has been reported that OPs show different pathways of degradation, depending primarily on their alkylation or arylation state and the nature of the nucleophile. For example, Bujan et al. studied the reactivity of *O,O*-dimethyl *O*-(3-methyl-4-nitrophenyl) phosphorothioate (Fenitrothion) in water with several O<sup>-</sup> and N<sup>-</sup>-based nucleophiles.<sup>8</sup> They found competition between the nucleophilic attack at the phosphorus atom and at the aliphatic carbon atom, S<sub>N</sub>2(P) and S<sub>N</sub>2(C), pathways, respectively, in the reactions with NH<sub>2</sub>OH. Nonetheless, the attack at the aliphatic carbon, S<sub>N</sub>2(C), is the main reaction pathway when Fenitrothion reacts with BuNH<sub>2</sub>.<sup>8</sup> In contrast, Buncel et al. found that the attack at the phosphorus center,

S<sub>N</sub>2(P), is the main pathway for the reactions of Fenitrothion with oximate nucleophiles in water.<sup>10</sup> However, for the reactions of Paraoxon and its sulfur analogue Parathion, the attack at the phosphorus center, S<sub>N</sub>2(P), has been reported as the sole reaction pathway.<sup>11</sup>

In the last 2 decades, ionic liquids (ILs) have been widely used as alternative reaction media for many organic reactions.<sup>12,13</sup> They have been shown to affect rates and reaction mechanisms, as well as product distribution in some reactions.<sup>12a</sup> However, some ILs have been used to prepare a series of phosphorodiamides and used for phosphorylation of nucleosides and 2-deoxynucleosides, demonstrating to be a versatile procedure with high product selectivity in comparison with their syntheses in conventional organic solvents (COS).<sup>14</sup> However, nothing has been reported, to our knowledge, concerning the effect of ILs on nucleophilic substitution reactions of phosphate esters.

To investigate the effects of ionic liquids as solvents on rate and product distribution of the nucleophilic substitution reactions of phosphoester compounds, in this work we study the reaction of *O,O*-diethyl 4-nitrophenyl phosphate triester (Paraoxon, **1**) with piperidine in ten ionic liquids, which are shown in Scheme 1. To compare the results obtained in ILs, we have carried out the same reaction in water, dioxane, acetonitrile, and DMSO under the same experimental conditions. The ILs used have a variety of cations and anions to allow investigation of the effects of the physicochemical properties of ILs on the reactivity of **1**. The kinetic experiments were followed through UV–vis and <sup>31</sup>P NMR techniques and the product analyses by <sup>31</sup>P NMR, UV–vis, and GC/MS.

Received: June 24, 2013

Published: September 3, 2013

Scheme 1. Schematic Representation of the Reaction Studied and the Ionic Liquids (ILs) Used

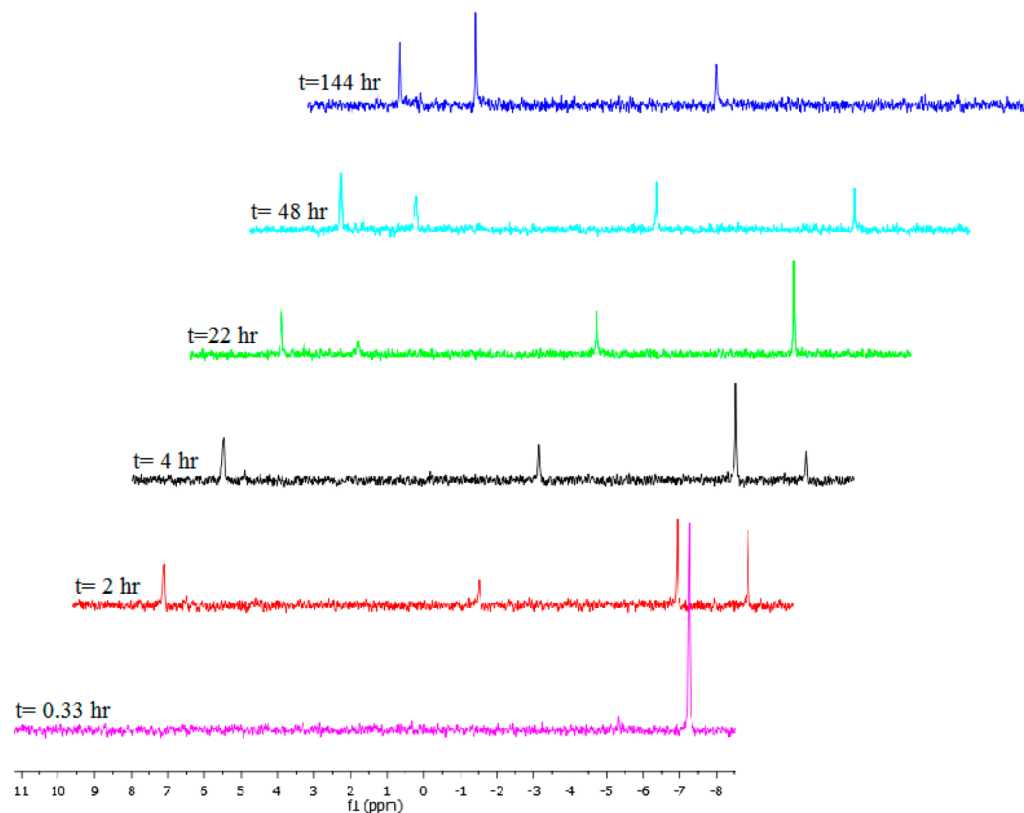
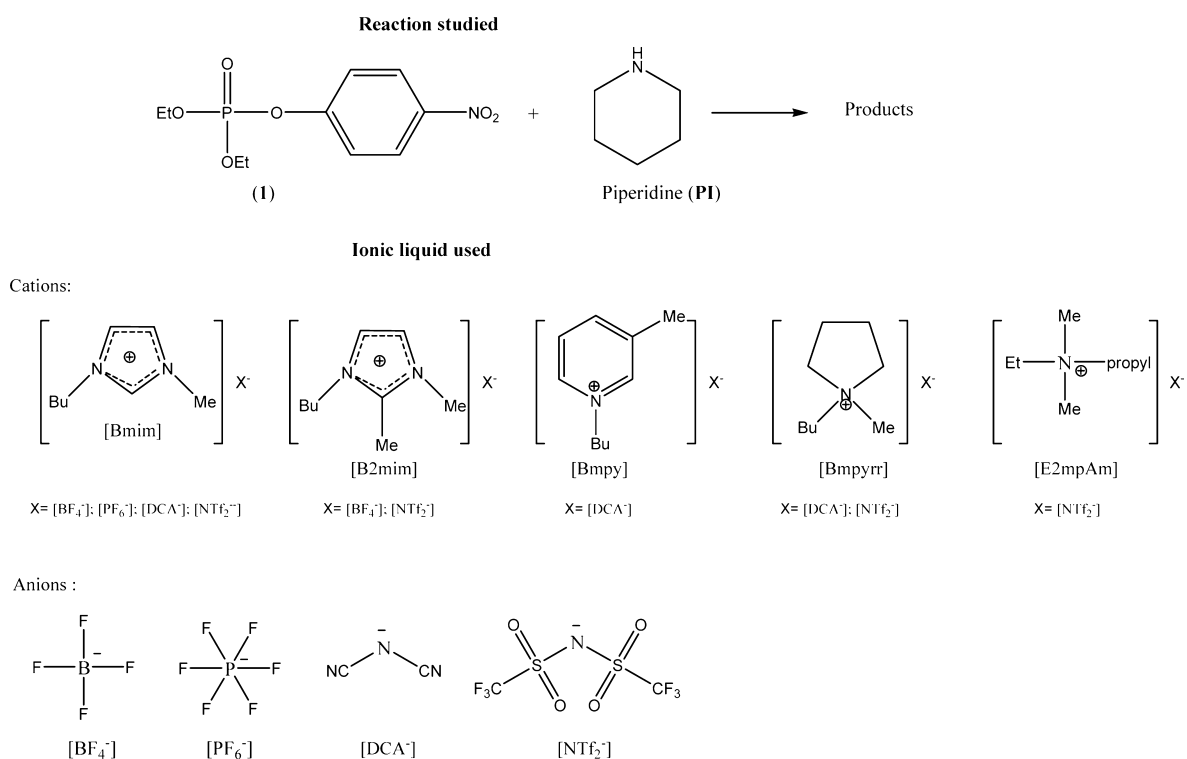


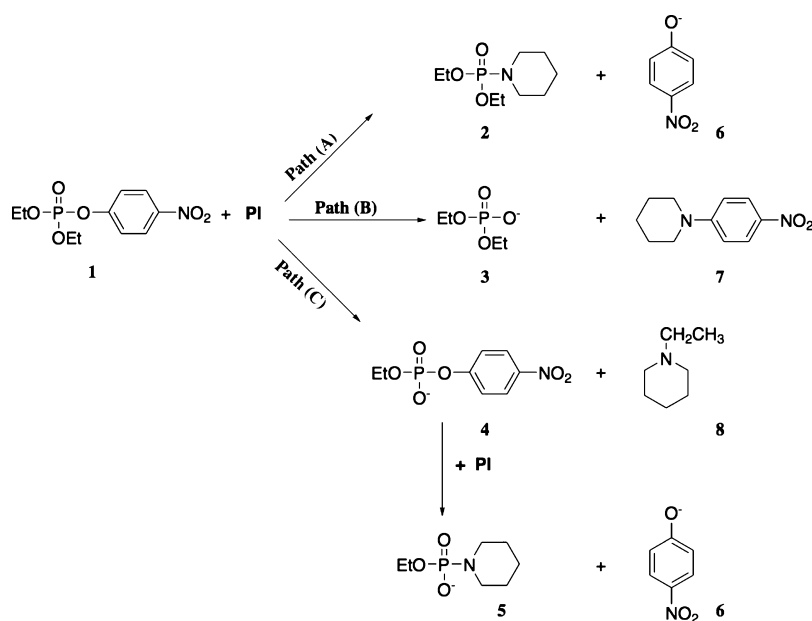
**Figure 1.** Progressive <sup>31</sup>P NMR spectra obtained for the reaction of **1** (0.01M) with piperidine (2.8 M) at 25 °C in [Bmim]DCA. The molar amounts corresponding to these spectra and others for this reaction are shown in Figure S14, in Supporting Information.

## RESULTS AND DISCUSSION

Figure 1 shows the <sup>31</sup>P NMR spectra of the reaction of **1** with piperidine in [Bmim]DCA solution at different times. As can be

observed, the decrease of substrate **1** signal (−7.3 ppm) is simultaneous to the increase of three other signals at 8.7, 0.1, and −5.3 ppm, which are assigned to the formation of some phosphorylated species in Scheme 2: *O,O*-diethyl piperidinophosphate

Scheme 2. Nucleophilic Attack of Piperidine (PI) to **1** in ILs and COS (Dioxane, ACN, and DMSO) by Three Reaction Paths: (A) At Phosphorus, (B) at the C-1 Aromatic Carbon, and (C) at the Aliphatic Carbon



diester (**2**), diethyl phosphate (**3**), and *O*-ethyl 4-nitrophenylphosphate diester (**4**), respectively. The peaks at 8.7 and 0.1 were assigned by comparison with the products obtained by the reactions of piperidine and NaOH with *O,O*-diethyl chlorophosphate in the same IL, respectively, as shown in Scheme S1 and Figures S1 and S2, in Supporting Information. On the other hand, the phosphate derivative **4** was identified by  $^{31}\text{P}$  NMR in comparison with an authentic sample; see Figure S3 in Supporting Information. (Synthesis details of **4** are shown in Experimental Section).

The presence of **2** among the reaction products (see Scheme 2) can be explained by the nucleophilic attack of piperidine to the phosphorus atom, where also the anion 4-nitrophenoxide (**6**) (leaving group) is formed: its presence was observed by the increase of a band at 420 nm in the UV-vis spectra. In addition, the nucleophilic attack to the C-1 carbon of the aromatic ring leads to compound **3** and 1-piperidino-4-nitrobenzene (**7**). The latter was determined by comparison of the UV-vis spectrum at the end of the reaction with that at the end of the reaction of 4-nitrochlorobenzene with piperidine at the same experimental conditions (in the 300–450 nm range).

The formation of **4** and *N*-ethylpiperidine (**8**) is observed when piperidine attack occurs at the aliphatic carbon, by the  $\text{S}_{\text{N}}2(\text{C})$  pathway. Compound **8** was identified by GC/MS (r.t. = 17.15 min,  $m/z$  113); see Figure S4 in Supporting Information. The reaction of **1** with piperidine showed a behavior similar to that in the other ionic solvents studied. Nevertheless, in COS the distribution of products (%) found was different. Figures S5–S17 in Supporting Information show the  $^{31}\text{P}$  NMR spectra recorded at different times in these solvents (note that for simplicity we do not show all the times recorded).

From analytical techniques (NMR, UV-vis, and GC/MS) we found that there are three simultaneous pathways to degradation of **1** in both COS and ILs as solvent. The three of them involve nucleophilic attack of piperidine at the following: (i) the phosphoryl center, resulting in P-Oaryl cleavage, (ii) the C-1 aromatic carbon, with aryl-O cleavage, and (iii) the aliphatic carbon, with alkyl-O breakage. These results are different to those previously

reported for degradation of **1** with different nucleophiles in aqueous solution, where the degradation of Paraoxon, caused by alkali metal ethoxides,<sup>15</sup> hydroxamate ions,<sup>11a</sup> and phenols and amines,<sup>11d</sup> occur by nucleophilic attack at the phosphoryl center as the only reaction pathway. This leads to the formation of 4-nitrophenoxide and the corresponding phosphate derivative. The nucleophilic attack at the aromatic and aliphatic carbons has not been reported for the reactions of Paraoxon. To have a better understanding of the reaction behavior in water solution, we carried out a  $^{31}\text{P}$  NMR study (see Figure S18 in Supporting Information) of this reaction using water as solvent under identical experimental conditions (temperature, concentration, and stoichiometry). Unfortunately, under these conditions, the pH was greater than 12 and an alkaline hydrolysis occurs, this being the main reaction pathway. Only minor products were found from the aminolysis reaction, which were also hydrolyzed later (see Figure S18 in SI). An external buffer was not used because the conditions would have been different than those in ILs.

However, the  $\text{S}_{\text{N}}\text{Ar}$  pathway found in this work is in accordance with previous investigations of nucleophilic aromatic substitutions in ionic liquids involving less activated aromatic rings. They include the *N*-arylation of secondary cyclic amines,<sup>16</sup> reactions of 2-substituted 5-nitrothiophenes,<sup>17</sup> and reaction of *p*-fluorobenzene with *p*-anisidine,<sup>18</sup> which reveals that  $\text{S}_{\text{N}}\text{Ar}$  reactions are favored when ILs are used as solvent.

It is worth mentioning that in the reaction of phosphate **1** with piperidine a new signal at 6.4 ppm is slowly appearing in the  $^{31}\text{P}$  NMR spectra (see Figure 1). As the reaction proceeds, the intensity of this signal increases at the expense of that of compound **4**, forming *O*-ethyl piperidinophosphate monoester (**5**) and **6**, due to a new piperidine attack to the phosphorus atom of **4** (see Scheme 2). This new compound **5** was confirmed on the basis of the increase of the same signal (6.4 ppm) in the reaction of *O*-ethyl 4-nitrophenyl phosphate monoester (**4**) with piperidine in the same experimental media (see Scheme S1 and Figure S15 in Supporting Information). This result is interesting from the toxicity point of view since it is known that phosphate

monoesters and diesters are much less lipophilic, and therefore less toxic, than their triester precursors.

However, the formation of 4-nitrophenoxide (**6**) in two different steps, as seen in Scheme 2, is evidenced by the shape of the absorbance vs time plot when the reaction of **1** with piperidine was followed by UV-vis at 420 nm; see Figure 2.

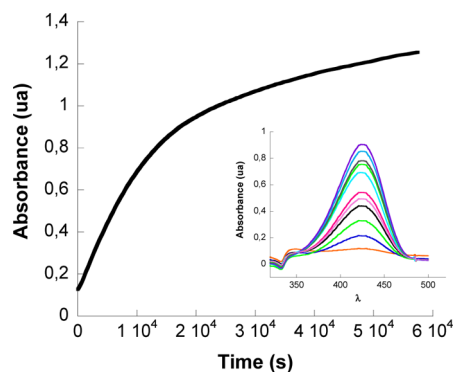


**Figure 2.** Experimental plot of absorbance (at 420 nm) vs time for the reaction of piperidine (0.4 M) with **1** in [Bmim]DCA at 25 °C. The inset shows the time-dependent UV-vis spectra of this reaction.

It can be seen that the curve in Figure 2 is not typical of a simple kinetic process. Its peculiar shape corresponds to at least two kinetically relevant steps responsible for the formation of **6**. This result confirms that 4-nitrophenoxide is formed in two consecutive steps, in agreement with the reaction scheme proposed (Scheme 2). Similar kinetic behavior (parallel and consecutive pathways) has been described and mathematically treated by an equation deduced by us in another system.<sup>19</sup>

However, from integration of the <sup>31</sup>P NMR signals of the products formed from piperidine attack to the different electrophilic centers of **1** (see Figures 1 and S5–S17), the relative products distribution was calculated in the different reaction media, as shown in Table 1. Figure 3 shows this behavior schematically.

**Table 1. Relative Products Distribution (%) for the Nucleophilic Attack of Piperidine to **1** in the Solvent Used**

|    | solvent                              | % S <sub>N</sub> 2(P) | % S <sub>N</sub> Ar | % S <sub>N</sub> 2(C) |
|----|--------------------------------------|-----------------------|---------------------|-----------------------|
| 1  | [Bmim]BF <sub>4</sub>                | 22                    | 19                  | 59                    |
| 2  | [Bmim]DCA                            | 33                    | 21                  | 46                    |
| 3  | [Bmim]NTf <sub>2</sub>               | 15                    | 28                  | 57                    |
| 4  | [Bmim]PF <sub>6</sub>                | 16                    | 26                  | 58                    |
| 5  | [B <sub>2</sub> mim]NTf <sub>2</sub> | 20                    | 30                  | 50                    |
| 6  | [B <sub>2</sub> mim]BF <sub>4</sub>  | 17                    | 21                  | 62                    |
| 7  | [E2mpAm]NTf <sub>2</sub>             | 22                    | 23                  | 55                    |
| 8  | [Bmpyrr]NTf <sub>2</sub>             | 18                    | 27                  | 55                    |
| 9  | [Bmpy]DCA                            | 54                    | 12                  | 38                    |
| 10 | [Bmpyrr]DCA                          | 18                    | 29                  | 53                    |
| 11 | dioxane                              | 1                     | 13                  | 86                    |
| 12 | ACN                                  | 8                     | 15                  | 76                    |
| 13 | DMSO                                 | 37                    | 23                  | 40                    |

These results agree with studies that report that slight modifications in the ILs' cation or anion nature would induce selectivity changes of some reactions.<sup>20</sup> We can observe that in most of the ILs employed the S<sub>N</sub>2(C) pathway (black columns in Figure 3) is the most important route for degradation of substrate **1** (46–62%) and that the S<sub>N</sub>Ar pathway (white columns) is

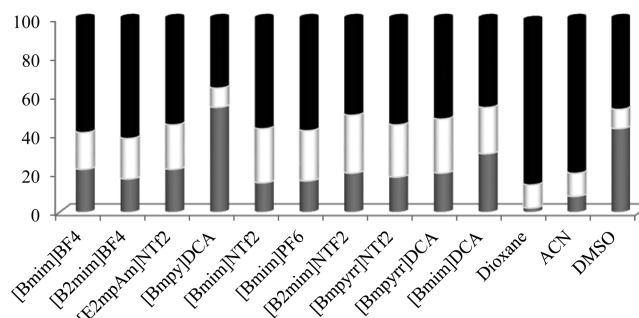


**Figure 3.** Relative nucleophilic attack of piperidine to **1** in ILs. Attack of piperidine at (gray columns) the phosphorus atom by S<sub>N</sub>2(P) pathway, (white columns) the C-1 aromatic carbon by the S<sub>N</sub>Ar pathway, and (black columns) the aliphatic carbon by the S<sub>N</sub>2(C) pathway.

almost independent of the ILs used (about 20%). Our results are very different from those reported for the same reaction in aqueous solution, in which the only reaction pathway is the attack of piperidine at the phosphorus atom.<sup>11</sup>

Interestingly, when [Bmpy]DCA is used as solvent, the S<sub>N</sub>2(P) pathway is the most important route for degradation of substrate **1** (54%). Also, we can observe that the change from [Bmpy]DCA to [Bmim]DCA and to [Bmpyrr]DCA results in a decrease of the percentage attack of piperidine to the phosphorus atom (from 54% to 33% and to 18%, respectively), entries 2, 9, and 10 in Table 1. The high preference for the S<sub>N</sub>2(P) pathway when the aromatic IL acts as solvent could be due to the stabilization of the transition state (TS) of this pathway by  $\pi$ - $\pi$  interactions of the aromatic cation with the TS, in comparison with compound **1**<sup>21</sup> (see kinetic results shown below).

To have control of the selectivity of this reaction, we have included three different conventional organic solvents (COS) in this study. Interestingly, the results of Table 1 show that, in the less polar COS, the selectivity is enhanced markedly at the aliphatic carbon atom and diminishes at the phosphorus atom of the substrate. Nevertheless, when DMSO is the solvent of the reaction, the selectivity is similar to that in ILs. This result is not surprising because, the same as ILs, the polarity and structure of DMSO lead to a considerable organization of the liquid state.<sup>22</sup> A similar trend has been reported previously by other authors when contrasting rate constants in DMF and ILs in the Kemp reaction<sup>20d</sup> and very recently by us in the aminolysis of aryl acetates in DMSO and ILs.<sup>23</sup>

However, we obtained pseudo-first-order rate coefficients ( $k_{\text{obsd}}$ ) for all the reaction routes (S<sub>N</sub>2(P), S<sub>N</sub>Ar, and S<sub>N</sub>2(C)), using the logarithmic plots of the <sup>31</sup>P NMR area, due to degradation of substrate **1** at different times, and the relative products distribution in Table 1. The  $k_{\text{obsd}}$  values found in the different media used in this study are shown in Table 2.

The results of Table 2 show that the  $k_{\text{obsd}}$  values found for the S<sub>N</sub>2(P) and S<sub>N</sub>Ar pathways in less polar solvent are lower than those in DMSO. These results could be rationalized in terms of the polarity-polarizability parameter of these solvents ( $\pi^* = 0.55, 0.75, \text{ and } 1.0$  for dioxane, ACN, and DMSO, respectively).<sup>24</sup> Although similar  $k_{\text{obsd}}$  values were found for DMSO and ILs for the three pathways, it is not adequate to compare these values on the grounds of polarity parameters, such as  $E_{\text{T}}(30)$ ,  $\epsilon$ , or  $\pi^*$ , because the interaction of substrates with ionic solvents seems to be affected by the complex structural organization of the ILs.<sup>25</sup>

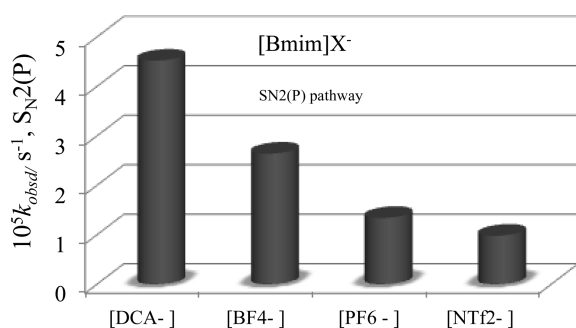
For the above reason, and to have a better understanding of our kinetic results, we resolved to discuss them as a function of the structure of the cation and anion of the IL.



**Table 2.** Pseudo-First-Order Rate Constants ( $k_{\text{obsd}}$ ) for the Degradation Routes of **1** in Several ILs and COS

| solvent                      | $10^5 k_{\text{obsd}}/s^{-1}$ ,<br>$S_N2(P)$ | $10^5 k_{\text{obsd}}/s^{-1}$ ,<br>$S_NAr$ | $10^5 k_{\text{obsd}}/s^{-1}$ ,<br>$S_N2(C)$ |
|------------------------------|--|--|--|
| [Bmim]BF <sub>4</sub>        | 2.64   | 2.28                                       | 7.08   |
| [Bmim]DCA                    | 4.52   | 2.88                                       | 6.30   |
| [Bmim]NTf <sub>2</sub>       | 0.99   | 1.85                                       | 3.78   |
| [Bmim]PF <sub>6</sub>        | 1.34   | 2.19                                       | 4.90   |
| [B2mim]NTf <sub>2</sub>      | 0.99   | 1.46                                       | 2.50   |
| [B2mim]BF <sub>4</sub>       | 0.82   | 1.00                                       | 3.01   |
| [E2mpAm]<br>NTf <sub>2</sub> | 0.74   | 0.77                                       | 1.84   |
| [Bmpyrr]NTf <sub>2</sub>     | 0.49   | 0.73                                       | 1.50   |
| [Bmpy]DCA                    | 5.15   | 0.95                                       | 0.34   |
| [Bmpyrr]DCA                  | 1.28   | 1.80                                       | 3.34   |
| Dioxane                      | 0.0064                                       | 0.083                                      | 0.55   |
| ACN                          | 0.17   | 0.33                                       | 1.65   |
| DMSO                         | 2.38   | 1.48                                       | 2.58   |

Figure 4 shows that the  $k_{\text{obsd}}$  values found for the  $S_N2(P)$  pathways with ILs that share a common cation decrease along the

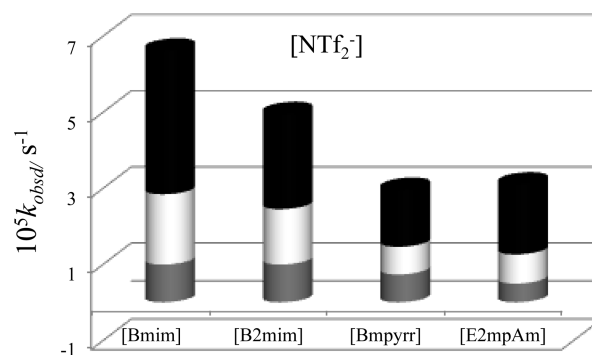
**Figure 4.** Variation of the pseudo-first-order rate coefficient ( $k_{\text{obsd}}$ ) with the nature of anion of the ionic liquid for the  $S_N2(P)$  pathway of the reaction of **1** with piperidine.

series: [Bmim]DCA > [Bmim]BF<sub>4</sub> > [Bmim]PF<sub>6</sub> > [Bmim]NTf<sub>2</sub>. The experimental trend seems to be in line with the hydrogen-bond acceptor (HBA) ability of the anion ( $\beta$  values of 0.708, 0.327, 0.202, and 0.23 for [Bmim]DCA, [Bmim]BF<sub>4</sub>, [Bmim]PF<sub>6</sub>, and [Bmim]NTf<sub>2</sub>, respectively).<sup>26,20d</sup> This indicates a stabilization of the transition state of the  $S_N2(P)$  pathway by the interaction between the IL anion and the hydrogen on the ammonium nitrogen of piperidine in the TS, facilitating the nucleophilic attack at the phosphorus atom of **1**.<sup>27</sup> Interestingly, for the  $S_NAr$  and  $S_N2(C)$  pathways the effect of the nature of the anion on the  $k_{\text{obsd}}$  value is less important.

As seen above, the  $k_{\text{obsd}}$  values for PF<sub>6</sub><sup>-</sup> and NTf<sub>2</sub><sup>-</sup> anions are not in accordance with their  $\beta$  values. This could be explained by the greater steric hindrance provided by the nitrogen anion of the bistrifluoromethylsulfonfyl group, (CF<sub>3</sub>SO<sub>2</sub>)<sub>2</sub>N<sup>-</sup>, (NTf<sub>2</sub><sup>-</sup>) in comparison with the hexafluorophosphate anion (PF<sub>6</sub><sup>-</sup>). Therefore, the HBA interaction with the N–H hydrogen of the TS would be lower.

To evidence the effect of the cation on the  $k_{\text{obsd}}$  values found along the three pathways for degradation of **1**, we performed a comparison of ILs that share a common anion (NTf<sub>2</sub><sup>-</sup>), as shown in Figure 5.

From this figure it follows that the highest  $k_{\text{obsd}}$  values are obtained when aromatic ILs are used. These results would suggest the highest  $\pi$  stacking interaction between aromatic

**Figure 5.** Variation of the pseudo-first-order rate coefficient ( $k_{\text{obsd}}$ ) for attack of piperidine at phosphorus by the  $S_N2(P)$  pathway (gray), the C-1 aromatic carbon by the  $S_NAr$  pathway (white), and the aliphatic carbon by the  $S_N2(C)$  pathway (black).

cation of the IL and the TS of the reaction, in comparison with the  $\pi$  stacking interaction between aromatic cation and reactants. In the case of [Bmim] and [B2mim] with a common anion (BF<sub>4</sub><sup>-</sup>), we found that the  $k_{\text{obsd}}$  value is two- to threefold greater when [Bmim]BF<sub>4</sub><sup>-</sup> is the reaction solvent. This result can be explained by the different hydrogen-bond donating (HBD) ability of the cations, suggesting that [Bmim] is a stronger hydrogen-bond donor than [B2mim], where position 2 is occupied by the methyl group.<sup>28</sup> In the case of [Bmim] and [B2mim], which share a common NTf<sub>2</sub><sup>-</sup>, we can observe a minimum effect. The latter results are in accordance with the  $r$  values reported by Armstrong et al.<sup>21</sup> The  $r$  values are 0 and 0.073 for [Bmim]NTf<sub>2</sub> and [B2mim]NTf<sub>2</sub>, respectively, at 40 °C.<sup>21</sup> The greater  $r$  value for the latter indicates that [B2mim] cation has a higher ability to interact with  $\pi$  electrons in comparison with [Bmim], providing [B2mim] with a greater aromaticity, stabilizing therefore, the TS of the reaction and increasing the  $k_{\text{obsd}}$  value. Therefore, in this case it is evident that both HBD ability and aromaticity of the ILs' cations must be taken into account to establish the effect of the cations nature on the  $k_{\text{obsd}}$  values.

Finally, it is clear that our analysis, by ignoring ion-pair interactions in these organic salts, and treating anions and cations as separate entities in these solvents, is not capable of uncovering all the subtle factors involved in such a complex system. Therefore, a better understanding of the ILs' effect could be explained taking into account the three-dimensional structure of ionic solvents, where solute–solvent interactions are much more complex.<sup>25</sup>

## CONCLUSIONS

An important conclusion from this study is the similar reactivity and selectivity of this reaction in DMSO and ILs used as solvent. Nevertheless, a marked difference exists with the behavior in less polar COS, where the selectivity is enhanced at aliphatic carbon atom and diminished at the phosphorus atom of the substrate.

In this study we found that both selectivity and rate constants ( $k_{\text{obsd}}$ ) depend on the nature of ILs' anion and cation. There is a correlation between  $\beta$  values of the anion and  $k_{\text{obsd}}$  values for the reaction, whereas the aromaticity of the cations seems to increase the rate of degradation of **1**. Nevertheless, we have found some exceptions, which make it necessary to take into account the three-dimensional structures of these solvents, which cover other factors involved in such a complex system.

It is noteworthy that the second reaction shown in Scheme 2 has not been described in the Paraoxon degradation. In this

reaction, the original substrate mainly yields a monoester derivative and the remaining corresponds to diethylphosphate and diethylpiperidinophosphate diester. Therefore, in this study it has been demonstrated that Paraoxon degradation is obtained with efficiency, yielding phosphate products less lipophilic and therefore less toxic to the human being.

## EXPERIMENTAL SECTION

**Materials.** All ionic liquids, conventional organic solvents (COS), piperidine, *O,O*-diethyl chlorophosphate, and *O,O*-diethyl 4-nitrophenyl phosphate triester (Paraoxon) were purchased. All ionic liquids were dried before use on a vacuum oven at 70 °C for at least 2 h and stored in a dryer under nitrogen and over calcium chloride. Water contents determined by Karl Fischer titration were <200 ppm.

*O*-Ethyl 4-nitrophenyl phosphate diester (**4**) was prepared by modification of a reported method,<sup>29</sup> as follows. 4-Nitrophenol (1.4 g, 10 mmol), *O,O*-diethyl chlorophosphate (1.72 g, 10 mmol), and triethylamine (1.11 g, 11 mmol) were dissolved in 50 mL of benzene. The solution was refluxed overnight and the precipitated triethylaminium hydrochloride was filtered. The benzene filtrate was extracted with water and dried over MgSO<sub>4</sub> and the benzene fraction was removed under reduced pressure to give Paraoxon. This was dissolved in 100 mL of acetone and refluxed for a day with dry LiBr (0.61 g, 7 mmol). The solution was left at 25 °C overnight and the precipitate was collected and washed with ether. After recrystallization from methanol/ether 1.05 g of pure compound **4** was obtained. <sup>1</sup>H NMR (400 MHz, DMSO  $\delta$ (ppm): 8.12 (d, 2H); 7.4 (d, 2H); 3.8 (“quintet”, 2H); 1.1 (t, 3H). <sup>13</sup>C-NMR (400 MHz, DMSO  $\delta$ (ppm): 16.6; 60.95; 120.4; 125.4; 141.8; 160.4. <sup>31</sup>P NMR (400 MHz, [Bmim]BF<sub>4</sub><sup>-</sup>)  $\delta$ (ppm): -5.6. Figure S3, in Supporting Information.

**Kinetic Measurements.** These were performed by <sup>31</sup>P NMR obtained on a 400 spectrometer, following the disappearing of the Paraoxon (**1**) signal. The kinetic experiments were carried out in ionic liquids and COS solutions at 25 °C under pseudo-first-order conditions. Each measurement was made in triplicate. In a typical experiment a NMR tube containing 500  $\mu$ L of the ionic liquid or COS was thermostatted at 25 °C for 10 min. Then Paraoxon ( $7.5 \times 10^{-6}$  mol, 15  $\mu$ L of 0.5 M in ACN) and piperidine ( $2 \times 10^{-3}$  mol, 200  $\mu$ L) were added. Deuterated ACN was used inserted in a capillary for NMR tubes. The spectra were recorded at different reaction times and pseudo-first-order rate coefficients ( $k_{\text{obsd}}$ ) were found for all reaction routes, S<sub>N</sub>2(P), S<sub>N</sub>Ar, and S<sub>N</sub>2(C). The overall  $k_{\text{obsd}}$  values were obtained by integration of the NMR signals for Paraoxon and plotting log (integration) vs time. To obtain the rate constants for the products formation, we multiplied  $k_{\text{obsd}}$  by the fraction of each product relative to the total products. The molar concentrations of the products at the end of the reactions were obtained by quantitative analysis of each product.

**Product Studies.** The product analysis was performed by different analytical techniques, as follows.

**Nuclear Magnetic Resonance.** To confirm the structural assignment of the products *O,O*-diethyl piperidine phosphate diester (**2**) and diethyl phosphate (**3**), <sup>31</sup>P NMR spectra were recorded for the reactions of *O,O*-diethyl chlorophosphate with piperidine and NaOH, respectively (see Scheme S1 and Figures S1 and S2). These reactions involve exclusive attack at the phosphoryl center. *O*-Ethyl 4-nitrophenyl phosphate diester (**4**) was prepared as described and product **5** was confirmed by comparison of an authentic sample with the <sup>31</sup>P NMR spectrum at the end of the reaction of **4** with piperidine (see Figure S19).

**Spectrophotometry.** The products 4-nitrophenoxide (**6**) and 1-piperidino-4-nitrobenzene (**7**), arising from the nucleophilic attack at the phosphoryl center and at the C-1 carbon of the aromatic ring, were identified by comparison of the final visible spectra of the reaction with an authentic sample (for **6**) and with the final spectra of the reaction of 4-nitro-1-chlorobenzene with piperidine (for **7**), in the ionic liquids. Typical UV-vis bands in the ionic liquids were found for compounds **6** and **7** at 420 and 325 nm, respectively (spectra not shown).

**Gas Chromatography–Mass Spectrometry (GC/MS).** GC/MS analysis was performed using a gas chromatograph fitted with a split-splitless injector and a Elite-5MS column (30 m  $\times$  0.25 mm i.d., 0.25  $\mu$ m d.f). Helium was used as a carrier gas at a flow rate of 1.0 mL/min. The injection port was maintained at 25.0 °C, and the split ratio was 19:1. Oven temperature was programmed from 70 °C for 2 min and then ramped as follows: ramp 1, 5 °C/min to 140 °C hold for 12 min, and ramp 2, 10 °C/min to 240 °C hold for 12 min. Ionization mode was electron impact ionization and the scanning range was from 50 to 400 amu. Mass spectra were obtained at 0.35 s intervals. To confirm the presence of *N*-ethylpiperidine (**8**) as a reaction product, an extraction with diethyl ether was made from the reaction medium and this extract analyzed by GC/MS; the spectrum obtained (see Figure S4) was matched with NIST library.

## ASSOCIATED CONTENT

### Supporting Information

Stacked <sup>31</sup>P NMR plot for the reaction of **1** with piperidine in ten ILs used and COS, GC/MS chromatogram, and mass spectrum of compound **7**. Experimental procedure, identification spectral data for compounds **2**–**5**. This material is available free of charge via the Internet at <http://pubs.acs.org/>.

## AUTHOR INFORMATION

### Corresponding Author

\*Tel.: +56-02-23541743. Fax: +56-02-26864744. E-mail: ppavezg@uc.cl

### Present Address

Facultad de Química, Pontificia Universidad Católica de Chile, Av. Vicuña Mackenna 4860, Santiago 6094411, Chile.

### Notes

The authors declare no competing financial interest.

## ACKNOWLEDGMENTS

This work was supported by project ICM-P10-003-F CILIS, granted by “Fondo de Innovación para la Competitividad” from Ministerio de Economía, Fomento y Turismo, Chile, and FONDECYT, grant 1130065.

## REFERENCES

- (1) Wu, T.; Gan, Q.; Jans, U. *Environ. Sci. Technol.* **2006**, *40*, 5428.
- (2) Casida, J. E.; Quistad, G. B. *Chem. Res. Toxicol.* **2004**, *17*, 983.
- (3) Chanda, A.; Khetan, S. K.; Banerjee, D.; Ghosh, A.; Collins, T. J. *J. Am. Chem. Soc.* **2006**, *128*, 12058.
- (4) Liu, B.; McConnell, L. L.; Torrents, A. *Chemosphere* **2001**, *44*, 1315.
- (5) Bravcon Kralj, M.; Cernigoj, U.; Franko, M.; Trebse, P. *Water Res.* **2007**, *41*, 4504.
- (6) Bravcon Kralj, M.; Franko, M.; Trebse, P. *Chemosphere* **2007**, *67*, 99.
- (7) Wanner, O.; Egli, T.; Fleischmann, T.; Lanz, K.; Reichert, P.; Schwarzenbach, R. P. *Environ. Sci. Technol.* **1989**, *23*, 1232.

- (8) Rougier, N. M.; Vico, R. V.; de Rossi, R. H.; Bujan, E. I. *J. Org. Chem.* **2010**, *75*, 3427.
- (9) (a) Pignatello, J. J.; Sun, Y. F. *Water Res.* **1995**, *29*, 1837.  
(b) Menger, F. M.; Rourk, M. J. *Langmuir* **1999**, *15*, 309.
- (10) Han, X. M.; Balakrishnan, V. K.; vanLoon, G. W.; Buncel, E. *Langmuir* **2006**, *22*, 9009.
- (11) (a) Ghosh, K. K.; Sinha, D.; Satnami, M. L.; Dubey, D. K.; Shrivastava, A.; Palepu, R. M.; Dafonte, P. R. *J. Colloid Interface Sci.* **2006**, *301*, 564. (b) Um, I. H.; Jeon, S. E.; Baek, M. H.; Park, H. R. *Chem. Commun.* **2003**, 3016. (c) Han, X. M.; Balakrishnan, V. K.; Buncel, E. *Langmuir* **2007**, *23*, 6519. (d) Castro, E. A.; Ugarte, D.; Rojas, M. F.; Pavez, P.; Santos, J. G. *Int. J. Chem. Kinet.* **2011**, *43*, 708.
- (12) (a) Welton, T. *Green. Chem.* **2011**, *13*, 225. (b) Welton, T. *Chem. Rev.* **1999**, *99*, 2071.
- (13) (a) Landini, D.; Maia, A. *Tetrahedron Lett.* **2005**, *46*, 3961. (b) Chowdhury, S.; Mohan, R. S.; Scott, J. L. *Tetrahedron* **2007**, *63*, 2363.
- (14) (a) Crossey, K.; Hardacre, C.; Migaud, M. E.; Norman, S. E. *RSC Adv.* **2012**, *2*, 2988. (b) Amigues, E. J.; Hardacre, C.; Keane, G.; Migaud, M. E.; Norman, S. E.; Pitner, W. R. *Green Chem.* **2009**, *11*, 1391. (c) Hardacre, C.; Huang, H.; James, S. L.; Migaud, M. E.; Norman, S. E.; Pitner, W. R. *Chem. Commun.* **2011**, *47*, 5846.
- (15) Um, I. H.; Shin, Y. H.; Lee, S. E.; Yang, K.; Buncel, E. *J. Org. Chem.* **2008**, *73*, 923.
- (16) Jorapur, Y. R.; Lee, C. H.; Chi, D. Y. *Org. Lett.* **2005**, *7*, 1231.
- (17) D'Anna, F.; Frenna, V.; Noto, R.; Pace, V.; Spinelli, D. *J. Org. Chem.* **2006**, *71*, 5144.
- (18) Newington, I.; Perez-Arlandis, J. M.; Welton, T. *Org. Lett.* **2007**, *9*, 5247.
- (19) Castro, E. A.; Cañete, A.; Campodónico, P. R.; Cepeda, M.; Pavez, P.; Contreras, R.; Santos, J. G. *Chem. Phys. Lett.* **2013**, *572*, 130.
- (20) (a) Cerda-Monje, A.; Aizman, A.; Tapia, R. A.; Chiappe, C.; Contreras, R. *Phys. Chem. Chem. Phys.* **2012**, *14*, 10041. (b) Wells, T. P.; Hallett, J. P.; Williams, C. K.; Welton, T. *J. Org. Chem.* **2008**, *73*, 5585. (c) D'Anna, F.; Marullo, S.; Vitale, P.; Noto, R. *ChemPhysChem* **2012**, *13*, 1877. (d) D'Anna, F.; La Marca, S.; Lo Meo, P.; Noto, R. *Chem.—Eur. J.* **2009**, *15*, 7896.
- (21) (a) Abraham, M. H. *Chem. Soc. Rev.* **1993**, *22*, 73. (b) Anderson, J. L.; Ding, J.; Welton, T.; Armstrong, D. W. *J. Am. Chem. Soc.* **2002**, *124*, 14247.
- (22) MacGregor, W. S. *Ann. N.Y. Acad. Sci.* **1967**, *141*, 3.
- (23) Millan, D.; Rojas, M.; Pavez, P.; Isaacs, M.; Diaz, C.; Santos, J. G. *New J. Chem.*, 10.1039/C3NJ00781B
- (24) Kamlet, M. J.; Abboud, J. L.; Taft, R. W. *J. Am. Chem. Soc.* **1977**, *99*, 6027.
- (25) (a) Dupont, J. J. *Braz. Chem. Soc.* **2004**, *102*, 85. (b) Dupont, J.; Suarez, P. A. Z. *Phys. Chem. Chem. Phys.* **2006**, *8*, 2441.
- (26) (a) Chiappe, C.; Pomelli, C. S.; Rajamani, S. J. *Phys. Chem. B* **2011**, *115*, 9653.
- (27) Crowhurst, L.; Lancaster, N. L.; Pérez Arlandis, J. M.; Welton, T. *J. Am. Chem. Soc.* **2004**, *126*, 11549.
- (28) (a) Köddermann, T.; Wertz, C.; Heintz, A.; Ludwig, R. *Chem. Phys. Chem.* **2006**, *7*, 1944. (b) Gozzo, F. C.; Santos, L. S.; Augusti, R.; Consorti, C. S.; Dupont, J.; Eberlin, M. N. *Chem.—Eur. J.* **2004**, *10*, 6187.
- (29) Moss, R. A.; Ihara, Y. *J. Org. Chem.* **1983**, *48*, 588.